Research article

Laboratory evaluation of alum, ferric and ferrous-water treatment residuals for removing phosphorous from surface water

George Carleton, Haidar Al daach, Teresa J. Cutright [*]

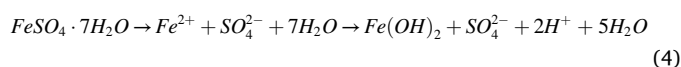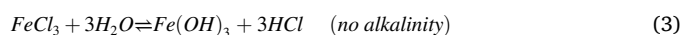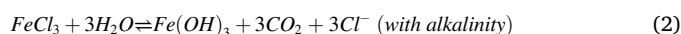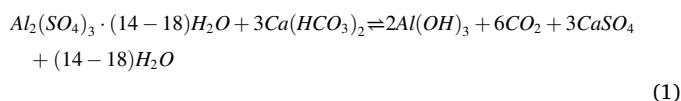Department of Civil Engineering, The University of Akron, Akron, OH, 44325-3905, USA

ABSTRACT

Numerous drinking water plants and agricultural wastewaters generate water treatment residuals (WTR) during coagulation processes. These WTRs may be effective at reducing nutrients entering waterways, thereby decreasing the potential formation of algal blooms. Of the WTRs used in this study, Al-based WTR (Al-WTR) was the most effective achieving a 20 °C cumulative adsorbed concentrations (q_e) after 28 days of desorption of 63–76 mg PO_4/kg Al-WTR depending on the initial spiked concentration. When the isotherm temperature was 5 °C, Al-WTR effectiveness decreased. Ferric chloride WTR (Fe-WTR) was only effective when 0.6 mg/L of PO_4 was spiked to surface water with 0.01 mg/PO_4 stored at 20 °C yielding a 28 day cumulative q_e 5.67 mg PO4/kg Fe-WTR. At 5 °C, the cumulative q_e after extended desorption was 1–4.63 mg/kg Fe-WTR. Ferrous sulfate based WTR (Fe2-WTR) was not capable of adsorbing any additional PO_4 regardless of the spiked concentration or temperature.

1. Introduction

There are two primary approaches to providing clean water: treating water so that it is safe for consumption and treating wastewater prior to release to a nearby waterway. A key step used to achieve these goals is coagulation and flocculation for removing suspended particles, dissolved inorganics and organic matter (Ahmad et al., 2017; Rivas et al., 2010). Although coagulation-flocculation processes are very effective, they produce substantial volumes of waste streams. In 2010, a 26 million gallon/day plant produced an average of 28,600 gal/day of water treatment residual (USEPA, 2011). Factoring in that most major cities have a drinking water plant, the global production of water treatment residual (WTR) is estimated at over 10,000 tons/day (Ahmad et al., 2017). However, drinking water plants are not the only source of WTRs. Cheese manufacturing, one of the primary agricultural products, produces a cheese-whey wastewater that contains very high levels of nitrogen and phosphorus (Carvalho et al., 2013). The treatment of cheese whey also produces significant wastewater residuals (Guerreiro et al., 2020). For instance, the European cheese industry produced 126,718 tons/yr of wastewater residuals (Ashekuzzaman et al., 2019). As there is a continuous generation of WTR from drinking water plants and cheese
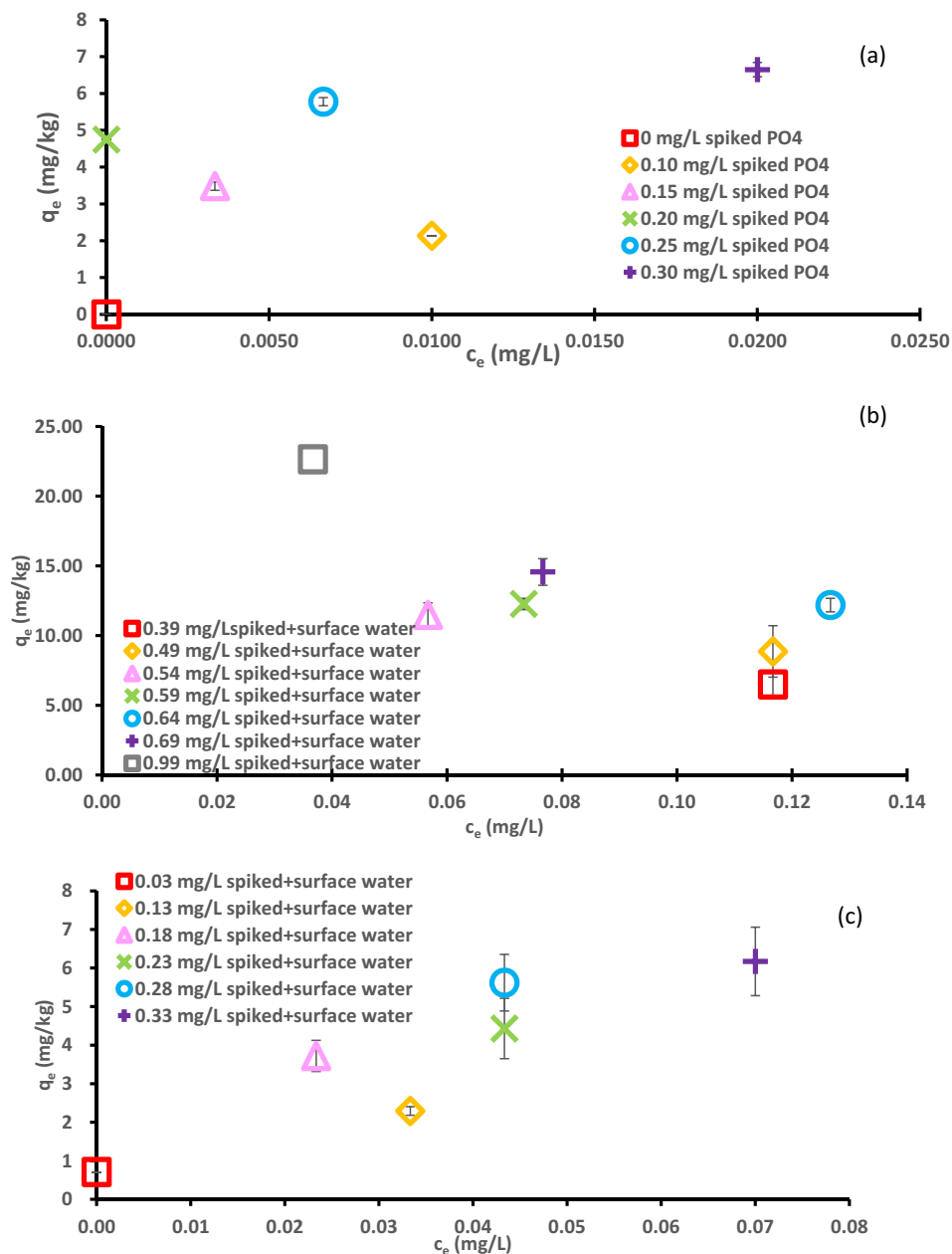
wastewater, finding a beneficial use for the WTRs would be advantageous.

The primary water/wastewater coagulants used are aluminum sulfate (alum), ferric chloride and ferrous chloride (Brennan et al., 2011; Matilainen et al., 2010). During coagulation treatment, the dominant reactions with alum, ferric chloride and ferrous chloride follow those shown in Eqs. (1), (2), (3), and (4) (Reynolds and Richards, 1996; Ebeling et al., 2003; Turner et al., 2019).

$$Al_2(SO_4)_3 \cdot (14-18)H_2O + 3Ca(HCO_3)_2 \rightleftharpoons 2Al(OH)_3 + 6CO_2 + 3CaSO_4 + (14-18)H_2O \tag{1}$$

$$FeCl_3 + 3H_2O \rightleftharpoons Fe(OH)_3 + 3CO_2 + 3Cl^- \ (with \ alkalinity) \tag{2}$$

$$FeCl_3 + 3H_2O \rightleftharpoons Fe(OH)_3 + 3HCl \quad (no \ alkalinity) \tag{3}$$

$$FeSO_4 \cdot 7H_2O \rightarrow Fe^{2+} + SO_4^{2-} + 7H_2O \rightarrow Fe(OH)_2 + SO_4^{2-} + 2H^+ + 5H_2O \tag{4}$$

Figure 1. Batch adsorption isotherm of PO$_4$ for Al-WTR with (a) distilled water at 20 °C with spiked concentration, (b) surface water with spiked concentration+0.39 mg/L background concentration at 20 °C and (c) surface water with the spiked concentration+0.03 mg/L background concentration at 5 °C. Error bars are standard deviation of triplicate samples.

Studies found that that the solids in the WTR have a strong adsorption capacity for reactive phosphorus (PO$_4$) as the WTR often contains substantial amounts aluminum or iron (Gao et al., 2013). Phosphorous adsorption capacities of 4.8–37 mg PO$_4$/g WTR have been achieved depending on the WTR used, contact time, and pH (Wang et al., 2011). The general reactions used to describe the adsorption of PO$_4$ onto Al-based and Fe-based WTR surfaces (Gibbons and Gagnon, 2011; Li et al., 2019; Yang et al., 2006) are given in Eqs. (5) and (6), respectively.

$$\equiv 2Al - OH + H_2PO_4^- \rightleftharpoons \equiv (Al)_2 HPO_4 + H_2O + OH^- \qquad (5)$$

$$\equiv Fe - OH + H_2PO_4^- \rightleftharpoons \equiv Fe - O - H_2PO_3 + OH^- \qquad (6)$$
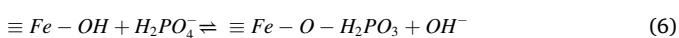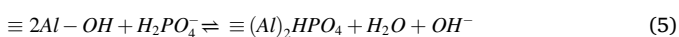
Most studies reported that ligand exchange was the dominant mechanism of PO$_4$ adsorption with OH flocs regardless of whether the WTR was alum or iron based (Gao et al., 2013; Zohar et al., 2017).

Additional reactions that are associated with the sorption capacity of WTR include hydroxide exchange, surface complexation, and co-precipitation (Xu et al., 2020).

As noted above, WTRs have an adsorption capacity for PO$_4$. However, the majority of the studies had processed the WTR before use. Pre-processing steps of sieving/grinding to a particle size of $\sim$ 2mm (Gao et al., 2013; Razali et al., 2007; Zohar et al., 2017), thermal treatment (Wang et al., 2016) or acid wash (Wang et al., 2011) have been done to increase the number of potential adsorption sites. These steps can add to the cost of using the WTR. The ultimate goal of the research sponsors was to use WTR the without any additional processing. Therefore, the objectives of this research were to conduct a preliminary evaluation on the i) feasibility of WTR that had not undergone preprocessing for reducing reactive phosphorous in surface waters, ii) impact of temperature on PO$_4$ sorption, and iii) differences between Al-based and Fe-based WTRs. It
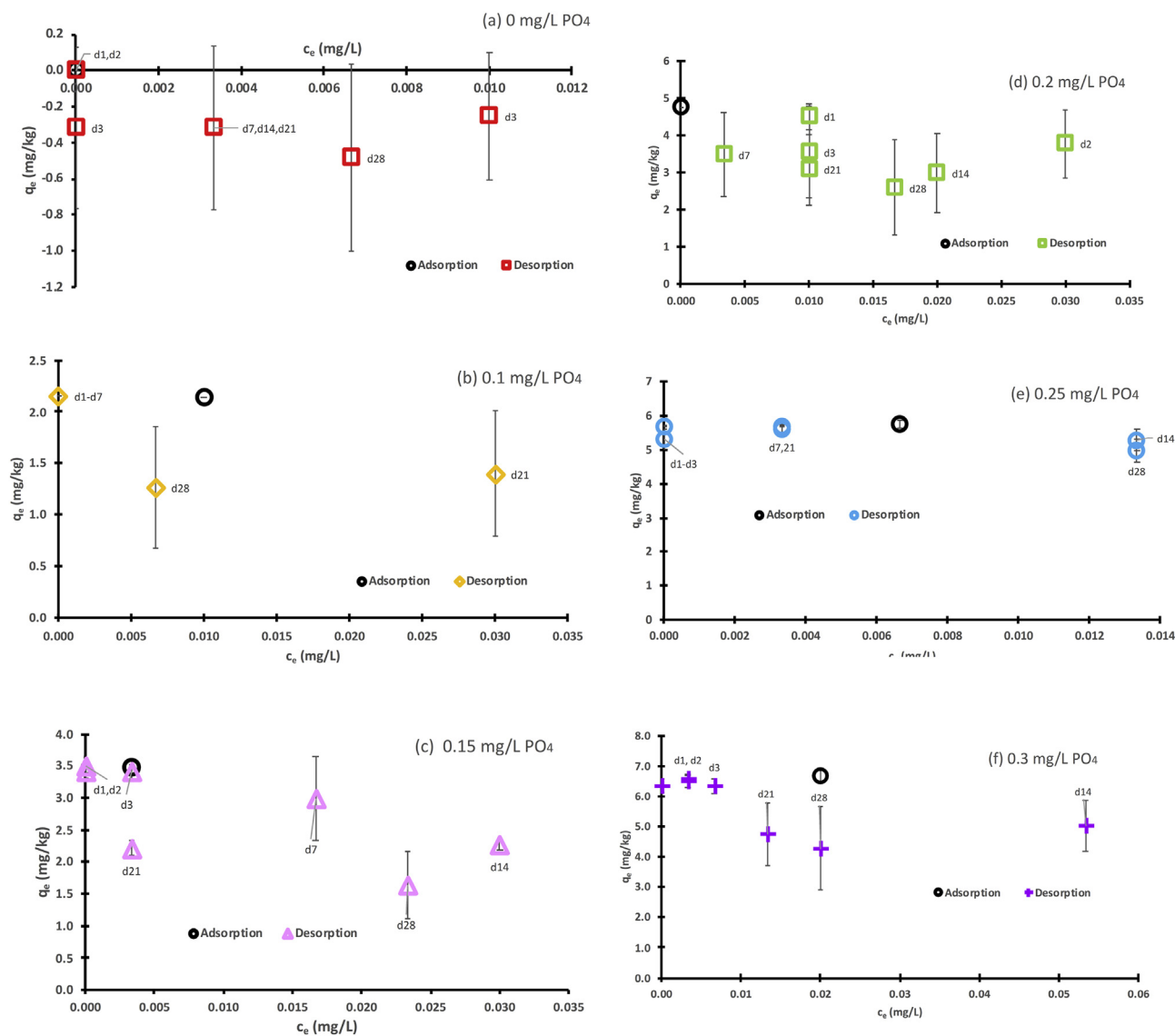
Figure 2. Al-WTR batch desorption isotherms with distilled water and stored statically at 20 °C for initial spiked PO4 concentration of: a) Control (0 mg/L spiked PO4); b) 0.10 mg/L spiked PO4; c) 0.15 mg/L spiked PO4; d) 0.20 mg/L spiked PO4; e) 0.25 mg/L spiked PO4; and f) 0.30 mg/L spiked PO4. Error bars are standard deviation of the triplicate samples. Data labels corresponds to the cumulative desorption day (i.e., d21 is cumulative desorption by day 21).

was hypothesized that Al-WTR and Fe-WTR would be more effective than ferrous-based WTR (Fe2-WTR).

2. Experimental methods

2.1. Water treatment residual sources, collection, and characterization methods

Three different WTRs were used in the study. Al-WTR was collected from drying beds of a 35 million gallon/day (MGD) drinking water plant located in northeast Ohio. Ferric-based WTR (Fe-WTR) was obtained from a 4.5 MGD drinking water plant in northeast Ohio. The ferrous-based WTR (Fe2-WTR) was collected from a cheese manufacturer that uses the coagulant to treat 600,000 gallon/day of dairy wastewater. WTRs were placed into separate clean buckets using clean shovels. Once filled, the buckets were sealed and transported to the laboratory. Aluminum leachate testing, iron leachate testing, and pH of each WTR were measured to establish baseline properties. The particle size of the WTRs was determined with U.S. standard sieves.

The potential initial release of target elements, Al or Fe, from the WTR upon re-wetting was assessed with 0.01 M $CaCl_2$ with a contact time of 72 h, 0.01 M $CaCl_2$ for 2 h, and distilled water with a contact time of 2 h (Maiz et al., 1997). All conditions used five replicates of 5 mg of WTR added to 50 mL of the appropriate solution. Flasks were sealed and placed in a Lab-Line Orbital Environ-Shaker at 50 rpm for the specified contact time. Afterwards, the flasks were decanted, filtered (Fisherbrand Q2 Filter Paper, particle retention >2 μm) and analyzed following the Aluminum Method 8012, Total Ferrover Method 8008 for ferric iron (Fe^{3+}) and Method 8146 for ferrous iron (Fe^{2+}, HACH, 2009) and a HACH DR 890 Colorimeter.

pH of the WTR samples were determined using 1:1 ratio of WTR to distilled water (Ippolito, 2015). Triplicate beakers containing 10 g of WTR and 10 mL of distilled water were stirred for 15 min. The supernatant pH was measured using a Fisher Scientific Education AccuTupH.

2.2. Surface water

Experiments with Al-WTR used surface water obtained from a tributary entering the drinking water reservoir. Fe-WTR isotherms used
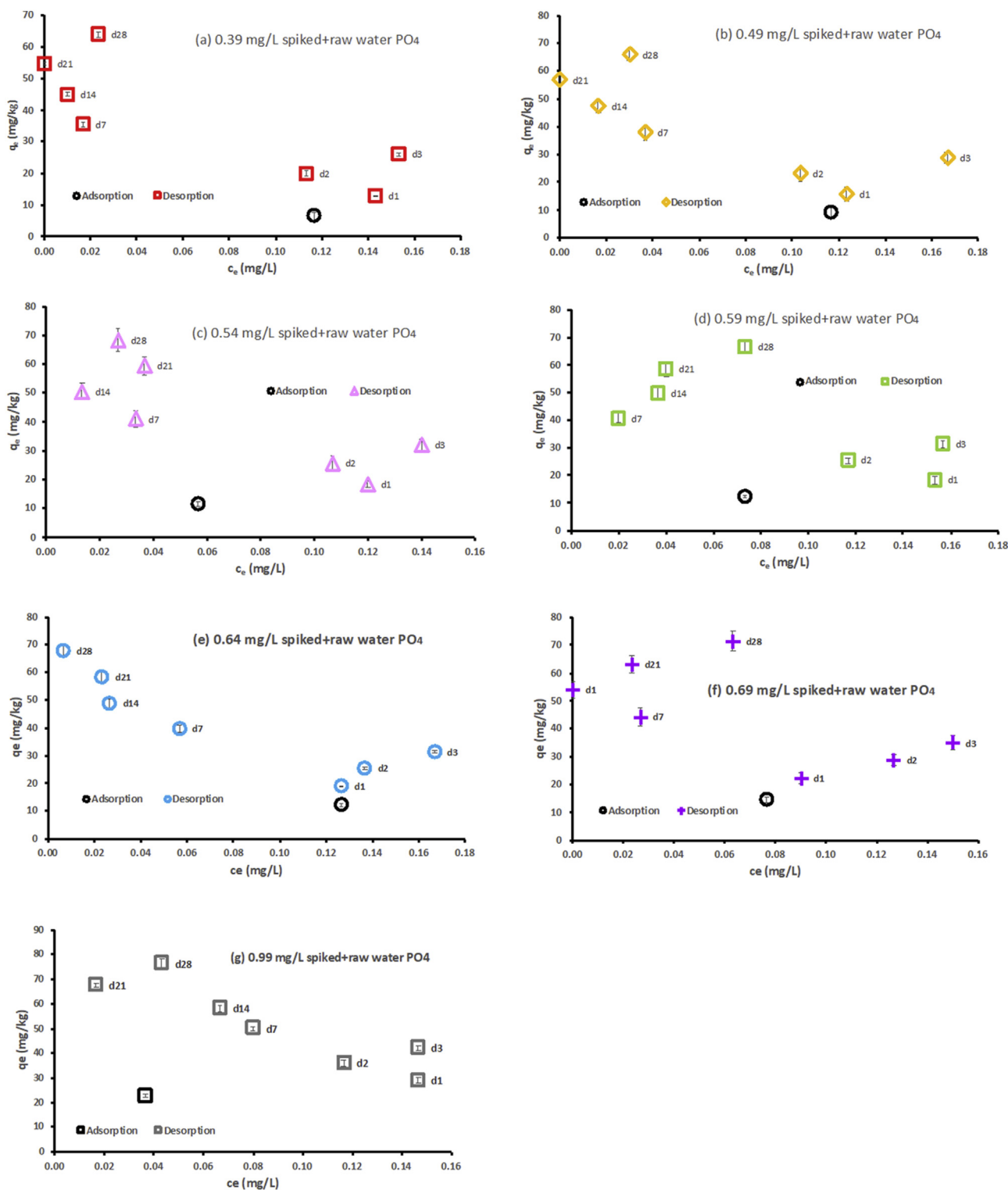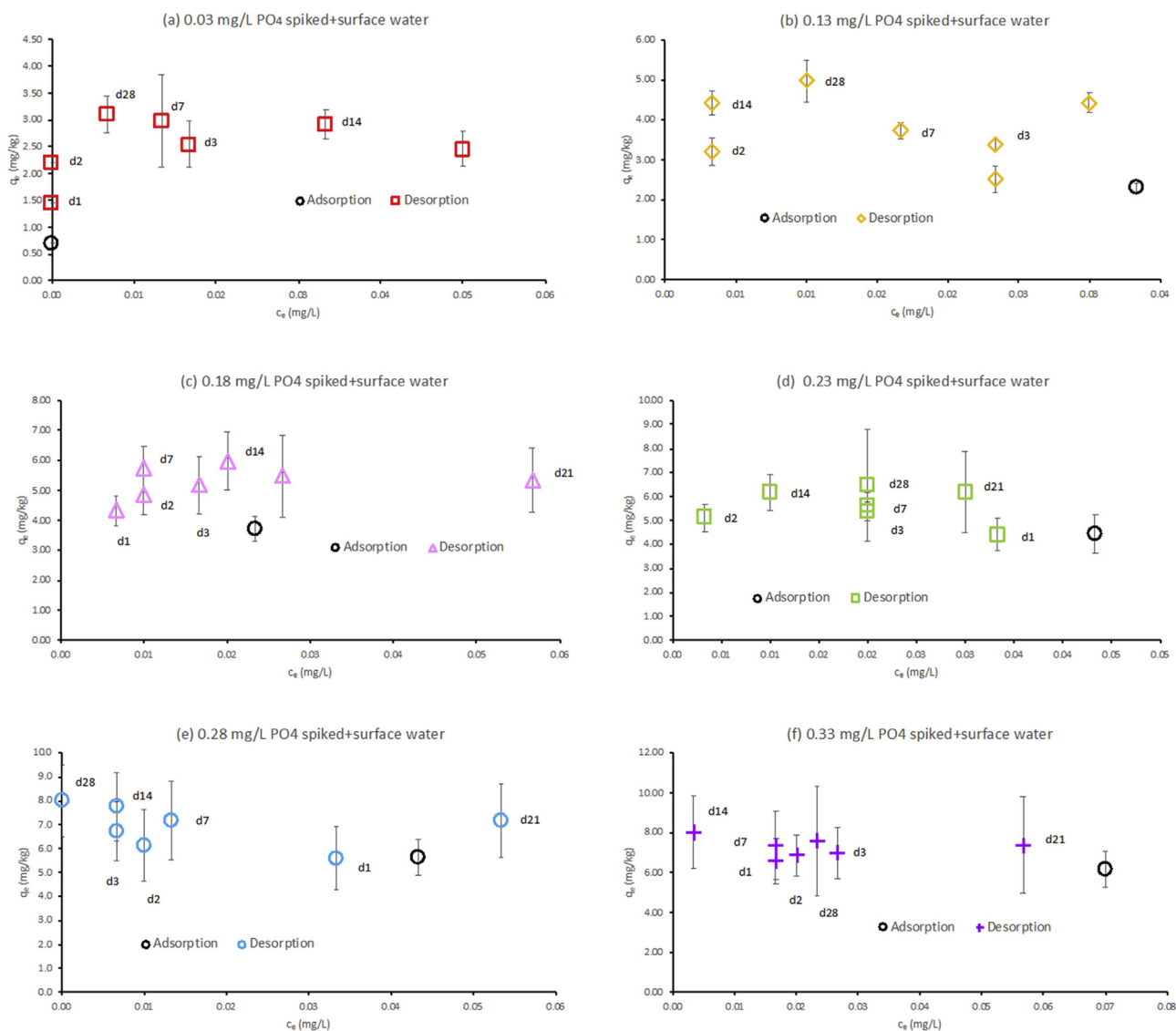
Figure 3. Al-WTR batch desorption isotherms with surface water containing 0.39 mg/L PO_4 and stored statically at 20 °C for initial spiked + surface water PO4 concentration of: a) Control (0.39 mg/L PO_4); b) 0.49 mg/L PO4, c) 0.54 mg/L PO4; d) 0.59 mg/L PO4; e) 0.64 mg/L PO4; f) 0.69 mg/L PO4; and g) 0.99 mg/L PO4. Error bars are standard deviation of the triplicate samples. Data labels corresponds to the cumulative desorption day.

surface water collected at the influent to the drinking water plant associated with the Fe-WTR. Fe2-WTR experiments used the surface water that the treated wastewater stream discharged to. For each collection, surface water was placed in clean buckets and transported to the lab. The PO4 levels were measured to determine the background concentration that would be added during the initial sorption phase and each refill during each desorption step. The background pH of each surface water

was determined using a pH probe (Fisher Scientific Education AccuTupH).

2.3. Adsorption-desorption isotherms

Batch sorption-desorption experiments used 1.6 g WTR to 40 mL of background solution in 40 mL glass vials. Depending on the specific

Figure 4. Al-WTR batch desorption isotherms with surface water containing 0.03 mg/L PO4 and stored statically at 5 °C for initial spiked + surface water PO4 concentration of: a) Control (0.03 mg/L PO4); b) 0.13 mg/L PO4, c) 0.18 mg/L PO4; d) 0.23 mg/L PO4; e) 0.28 mg/L PO4; and f) 0.33 mg/L PO4. Error bars are standard deviation of the triplicate samples. Data labels corresponds to the cumulative desorption day.

experimental set, the background solution was either: distilled water as a control to assess if any of the PO4 already present in the WTR would desorb; distilled water spiked with PO4 to determine the maximum that would adsorb-desorb without interferences; or surface water spiked with PO4 to mimic field conditions, assess the impact of impurities as well as simultaneous sorption-desorption. The addition of the spiked PO4 initiated the adsorption phase.

Three experimental sets were conducted for each WTR: distilled water at 20 °C, surface water at 20 °C and surface water at 5 °C. Each experimental set consisted of seven sets of triplicate reactors spiked at 0 (control), 0.10, 0.15, 0.20, 0.25, 0.30, and 0.60 mg/L of reactive PO4 to mimic influent conditions at the drinking water plants. The initial spiked reactive PO4 concentration used to initiate the experiment was the only time that the samples were spiked. It is important to note that the 0.6 mg/L PO4 with distilled water and Al-WTR was initially omitted. After 24 h, the background solution was decanted, filtered through 2 μm filter (Fisherbrand Q2), and analyzed for reactive PO4 following the Reactive Phosphorus PhosVer 3 Method 8048 (HACH, 2009).

Immediately after the background solution used in the sorption phase was decanted, fresh background solution with the same composition as solution used in sorption phase was added to begin the

desorption phase of the experiment. Desorption was measured at contact times of 1, 2, 3, 7, 14, 21, and 28 days. At each time interval, the background solution was decanted for analysis, and new background solution was added. The first day was used as the traditional equilibrium 24-hr time step. Days 2, 3, 7, 14, 21, and 28 were used to assess the simultaneous adsorption-desorption that could occur when surface water was used (Hale et al., 2013).

The adsorbed concentration, q_e (mg/kg), for the adsorption phase was found by:

$$q_e = \frac{[c_i - c_e]*v}{m} \tag{7}$$

For the desorption phase of the experiment, Eq. (7) was modified to:

$$q_e = q_{e-1} + \frac{[c_B + c_{e-1}*(1 - R) - c_e]*v}{m} \tag{8}$$

where c_i is the initial reactive PO4 concentration (mg/L), c_e is the measured equilibrium solution concentration (mg/L), v is the volume of background solution (L), and m is the mass of sorbent (kg). Additional parameters in Eq. (8) were c_B the reactive PO4 concentration of the
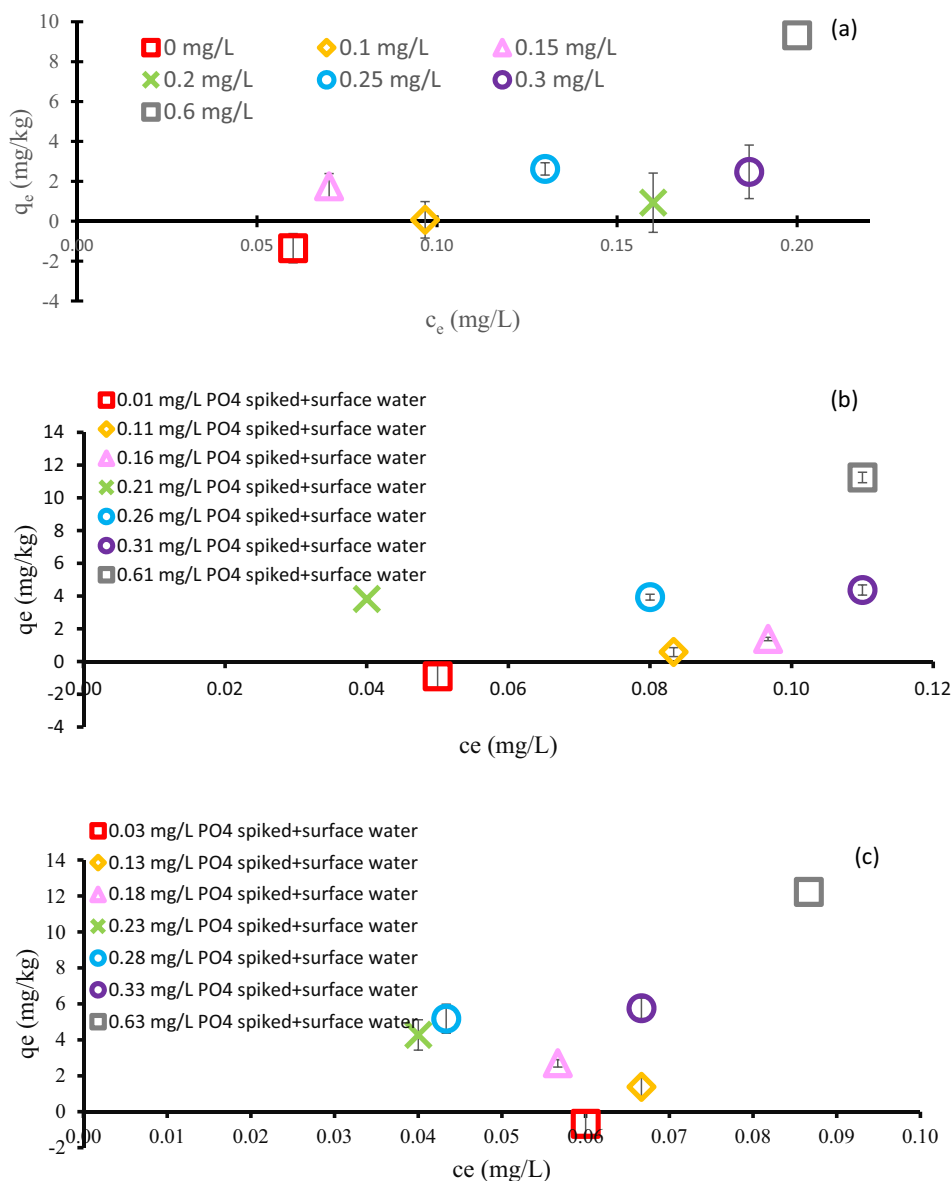
Figure 5. Batch adsorption isotherm of PO4 for ferric-chloride-based WTR (Fe-WTR) with (a) distilled water at 20 °C with spiked concentration, (b) surface water with spiked concentation+0.01 mg/L background concentration at 20 °C and (c) surface water with the spiked concentration+0.03 mg/L background concentration at 5 °C. Error bars are standard deviation of triplicate samples.

background solution (mg/L), c_{e-1} is the equilibrium concentration of the previous sorption step, and R is the fraction of supernatant replaced. All batch isotherms experiments had a v of 0.04 L, m of 0.016 kg, and R value of 0.95.

After the adsorption phase qe's were calculated (equation 7), the data were fitted to determine the kinetic coefficients. This was only possible for the adsorption phase as desorption phase with surface water introduced new PO4 at each refill step. The data was evaluated with both the Langmuir and Freundlich equations models. The q_m and K_{ads} in the Langmuir Eq. (9) are the maximum capacity of the WTR (i.e., adsorbent) for PO4 (adsorbate), respectively (Reynolds and Richards, 1996; Cheng et al., 2017). For the Freundlich equation (10),K is a measure of the adsorption capacity (mass adsorbate/mass adsorbent) and n is an indication of how the affinity of the adsorbate changes with changes in the amount adsorbed (Reynolds and Richards, 1996; Cheng et al., 2017). In both equations, q_e and c_e are the adsorbed concentration and aqueous phase concentration, respectively.

$$q_e = q_m \frac{K_{ads}c_e}{1 + K_{ads}c_e} \tag{9}$$

$$q_e = Kc_e^{1/n} \tag{10}$$

2.4. Statistical analysis

Three factor analysis of variance (ANOVA) and Tukey comparison test with 95% confidence were used to analyze the differences between the varying batch isotherm conditions using Minitab (version 18.1). The factors were WTR source (Al-, Fe- and Fe2-WTR), isotherm condition (temperature and background solution), and spiked PO4 concentration. The response variables for comparison of the factors were the cumulative day 28 desorption q_e values and change in q_e values from the 24-hr adsorption to the cumulative day 28 desorption step. Responses with p < 0.05 were statistically significant.
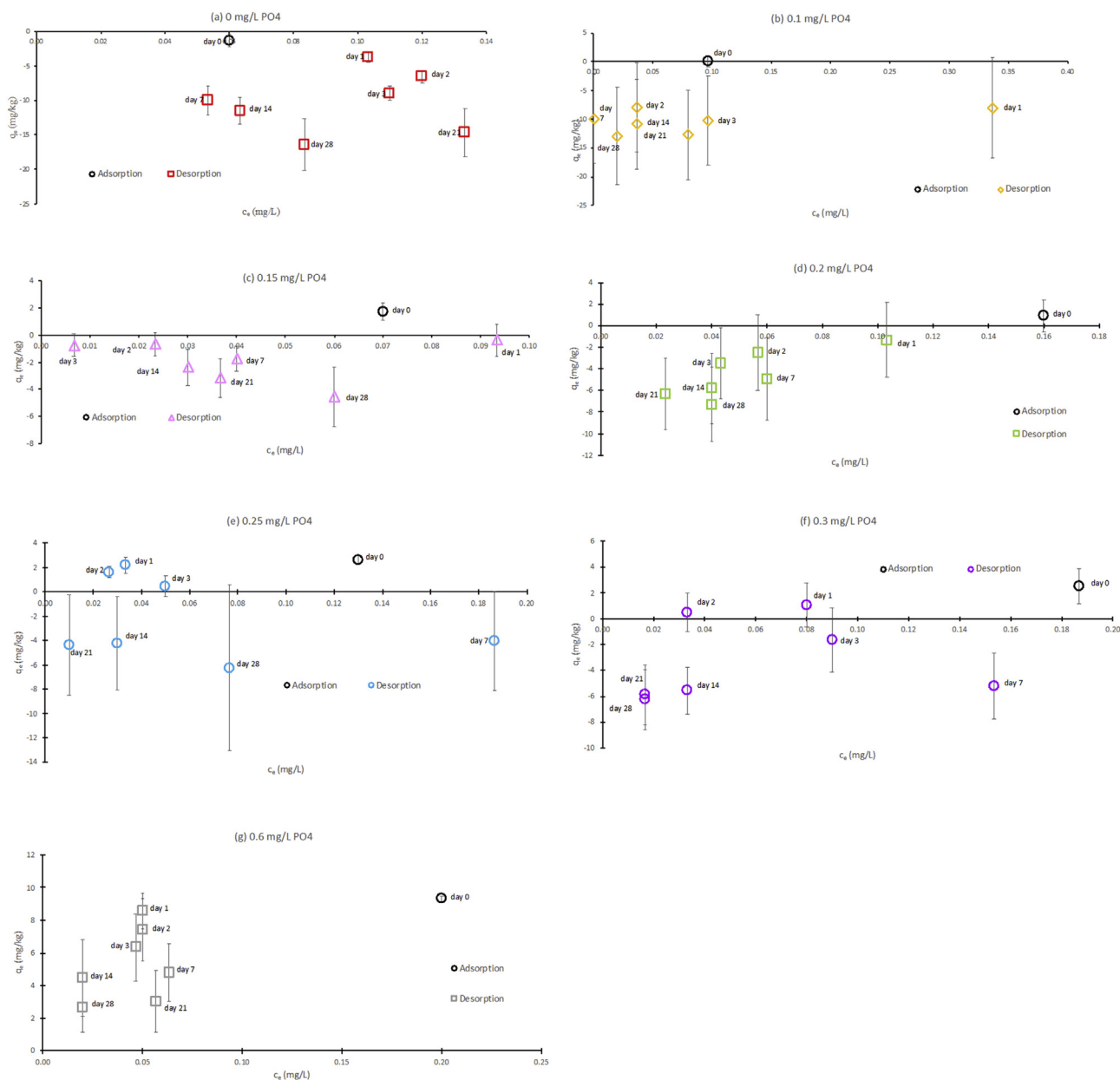
Figure 6. Fe-WTR batch desorption isotherms with distilled water and stored statically at 20 °C for initial spiked PO4 concentration of: a) Control (0 mg/L spiked PO4); b) 0.10 mg/L spiked PO4; c) 0.15 mg/L spiked PO4; d) 0.20 mg/L spiked PO4; e) 0.25 mg/L spiked PO4; f) 0.30 mg/L spiked PO4 and g) 0.6 mg/L spiked PO4. Error bars are standard deviation of the triplicate samples. Data labels corresponds to the cumulative desorption day (i.e., d21 is cumulative desorption by day 21).

## 3. Results and discussion

3.1. Characteristics of WTRs

The Al-WTR was 29.11% gravel (4.75–75 mm), 62.43% sand (0.075–4.75 mm) and 0.11% silt and clay (<0.75 mm). The potential initial amount of aluminum that released when distilled water was used 0.019 ± 0.025 mg Al/L. A 2-hr contact with $CaCl_2$ yielded the same result of 0.018 ± 0.028 mg/Al ($p > 0.05$) while the 72 h contact time leached slightly ($p > 0.05$) more aluminum 0.026 ± 0.020 but was still within the acceptable range (0.63–3,200 µg/L) for the USEPA (2018) aquatic life criterion. The pH value for the Al-WTR was 6.99 ± 0.21. This was similar to the results of Dayton and Basta (2001) who reported an average pH for Al-WTR to be 7.1.

The Fe-WTR 11.55% gravel, 62.99% sand and 21.05% silt/clay. The pH was 7.32 ± 0.07. Assessing the leaching release of Fe upon rewetting was important as it will impact the efficiency of

the WTR to be beneficially reused. With distilled water as the background solution, 0.54 ± 0.03 mg/L Fe was released. $CaCl_2$ solution released the same amount of Fe regardless of whether the contact time was 2 h (5.31 ± 0.38 mg/L Fe) or 72 h (4.65 ± 1.16 mg/L Fe) ($p > 0.05$).

Fe2-WTR had the largest particle sizes with 69.35% gravel, 27.35% sand and 1.45% silt/clay. As particle size WTRs with a smaller mean particle size can absorb greater amounts of PO4 (Turner et al., 2019), this may impact the extent of adsorption during isotherm experiments. The Fe2-WTR depicted a greater fluctuation in Fe content for the five replicates. The distilled water solution released 0.04 ± 0.05 mg/L Fe while the 2 h $CaCl_2$ and 72 h $CaCl_2$ released 0.02 ± 0.05 mg/L Fe and 0.03 ± 0.02 mg/L Fe, respectively ($p > 0.05$). The average pH of the Fe2-WTR was 7.09 ± 0.06.

None of the WTRs had a pH outside the optimum range 0f 6.5–8.5 for most aquatic organisms (USEPA, 2018). This indicated that they would not pose detrimental effects associated with pH.
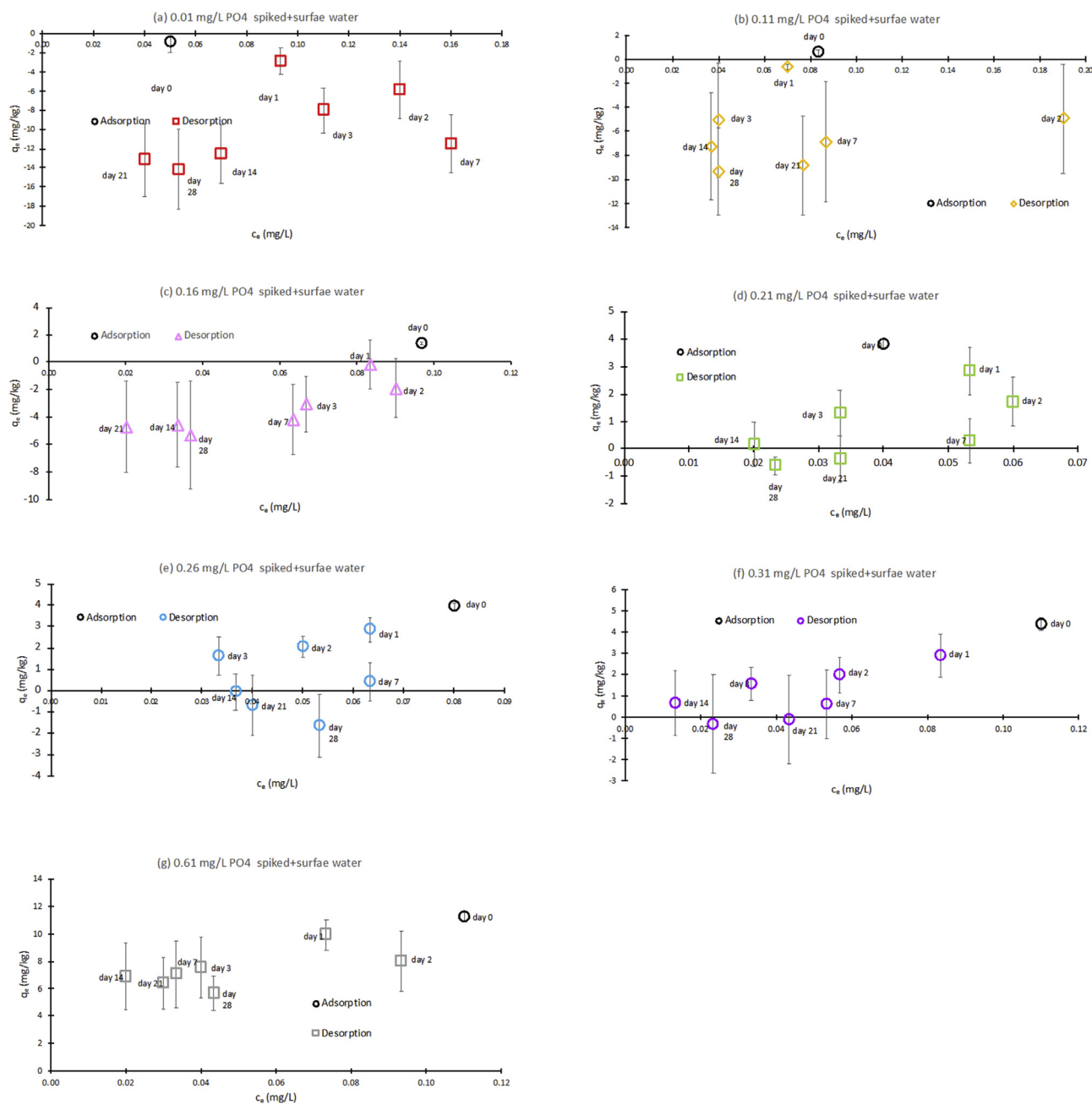
Figure 7. Fe-WTR batch desorption isotherms with surface water containing 0.01 mg/L PO4 and stored statically at 20 °C for initial spiked PO4 concentration of: a) Control 0.01 mg/L PO4 spiked + surface water; b) 0.11 mg/L spiked + surface water PO4; c) 0.16 mg/L spiked + surface water PO4; d) 0.21 mg/L spiked + surface water PO4; e) 0.26 mg/L spiked + surface water PO4; f) 0.31 mg/L spiked + surface water PO4, and g) 0.61 mg/L spiked + surface water PO4. Error bars are standard deviation of the triplicate samples. Data labels corresponds to the cumulative desorption day (i.e., d21 is cumulative desorption by day 21).

The particle size of the WTRs were different. As mentioned above, the dominant size for the Al- and Fe-WTR was 0.075–4.75 mm while the Fe2-WTR was predominantly >4.75 mm. The smaller particle size with Al-WTR and Fe-WTR provides a higher surface area; which could lead to a higher sorption capacity (Bacelo et al., 2020; Caporale et al., 2013).

3.2. Al-WTR adsorption-desorption isotherms

Figure 1 contains the amount of reactive PO4 that was adsorbed by Al-WTR after 24 h. In general, as the spiked PO4 concentration increased, the amount adsorbed to the Al-WTR (q_e) increased. For instance, when distilled water was the background solution (Figure 1a), the 0.1 mg/L

PO4 spiked condition yielded a q_e of 2.14 mg/kg Al-WTR and aqueous phase concentration (c_e) of 0.01 mg/L while 0.3 mg/L spiked condition adsorbed 6.65 mg/kg Al-WTR and 0.02 mg/L c_e. Significantly higher q_e's ($p < 0.05$) were achieved during the sorption with surface water (Figure 1b). This was expected as the surface water contained 0.39 mg/L PO4. Therefore, the amount of PO4 present during the adsorption phase was the 0.39 mg/L present in the surface water plus the spiked concentration. The PO4 concentration in the surface water used for the 5 °C experiments was 0.03 mg/L (Figure 1c). Although this led to similar adsorption values when distilled water (Figure 1a) was the background solution, the c_e was higher ($p < 0.05$). Overall, the extent of adsorption was in line with Zohar et al. (2017) study where Al-WTR removed more than 80% of phosphorus (organic or inorganic).
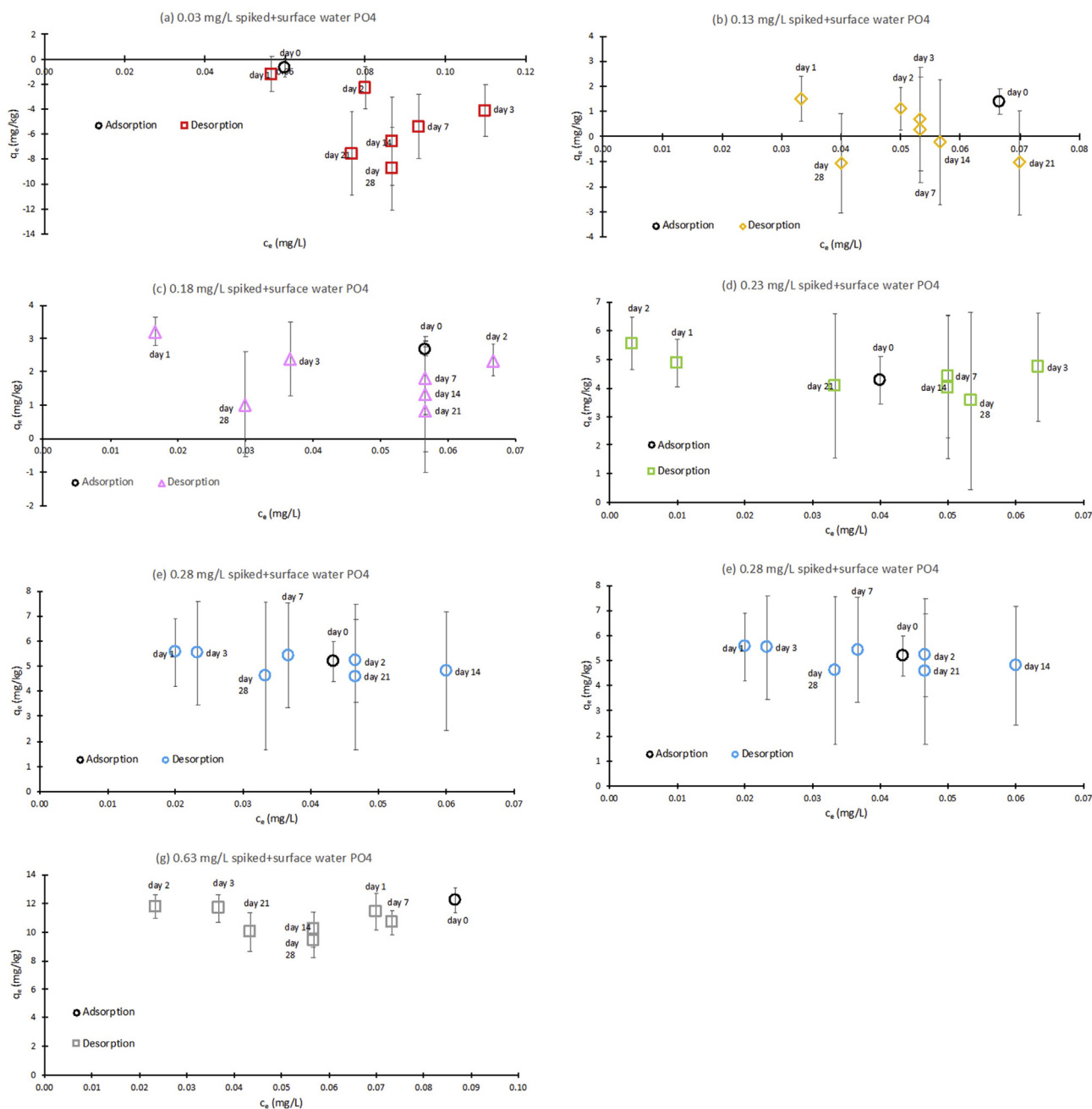
Figure 8. Fe-WTR batch desorption isotherms with surface water containing 0.03 mg/L PO_4 and stored statically at 5 °C for initial spiked PO4 concentration of: a) Control 0.03 mg/L PO_4 spiked + surface water; b) 0.13 mg/L spiked + surface water PO4; c) 0.18 mg/L spiked + surface water PO4; d) 0.23 mg/L spiked + surface water PO4; e) 0.28 mg/L spiked + surface water PO4; f) 0.33 mg/L spiked + surface water PO4, and g) 0.63 mg/L spiked + surface water PO4. Error bars are standard deviation of the triplicate samples. Data labels corresponds to the cumulative desorption day (i.e., d21 is cumulative desorption by day 21).

As mentioned earlier, with distilled water background solution, PO_4 was added only added to initiate the 24 h sorption and desorption phase began immediately after the 24 h sorption. The control set (Figure 2a, no spiked PO_4) desorbed some of the PO_4 that was sorbed when alum was added as a coagulant during water treatment. This was attributed to a reverse concentration gradient effect that occurs when the concentration of the target in solution is less than that adsorbed to the sorbent (Corwin and Summers, 2011). Even with spiked PO_4 concentrations, the distilled water experiments exhibited PO_4 desorption during each successive desorption step. For example, the 0.15 mg/L spiked condition (Figure 2c) had a q_e of 3.49 mg/L PO_4/kg AL-WTR after the first desorption step that decreased to a q_e of 1.65 mg/kg Al-WTR by day 28.

As expected, Al-WTR exhibited less desorption when surface water was used. The 'fresh' PO_4 added during each refill of background solution provided more PO_4 to simultaneously adsorb-desorb which minimized the reverse concentration gradient effect. The control surface water condition (0.39 mg/L PO_4 Figure 3a) depicted a q_e of 63.93 mg PO_4/kg Al-WTR by the day-28 desorption step. When the combined spiked (0.6 mg/L) and surface (0.39 mg/L) concentration was 0.99 mg/L (Figure 3g), the q_e for the 28-day cumulative desorption was 76.24 mg PO_4/kg Al-WTR with an aqueous phase c_e of 0.04 mg/L PO_4 (p < 0.05).

When the isotherm temperature was decreased to 5 °C to mimic late fall conditions, the amount of PO_4 released during desorption steps increased. Extent of desorption was more pronounced at lower spiked
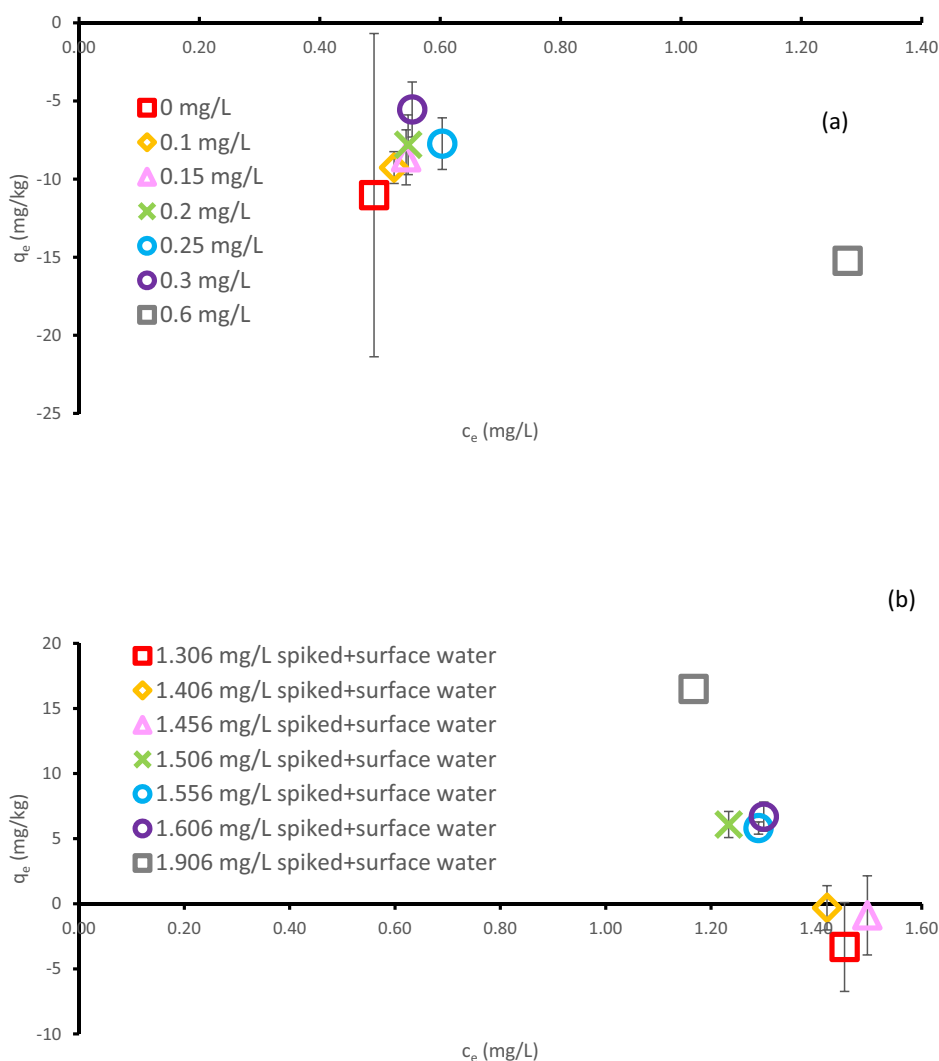
Figure 9. Batch adsorption isotherm of PO$_4$ for Ferrous-WTR (Fe2-WTR) with (a) distilled water with spiked concentration and (b) surface water with the spiked concentration+1.306 mg/L background concentration. Error bars are standard deviation of triplicate samples.

concentrations. Figure 4b shows that the cumulative q$_e$ at day 28 desorption step was 4.96 mg PO$_4$/kg Al-WTR. As 0.03 mg/L was added at each desorption step, the total PO$_4$ in contact with Al-WTR was 0.013 mg, the q$_e$ corresponds to a 61.7% removal. With a combined 0.28 mg/L spiked (0.25 mg/L) and surface water (0.03 mg/L) concentration, the total PO$_4$ in solution with time was 0.02 mg. Therefore, the Al-WTR day 28 q$_e$ of 8.0 mg PO$_4$/kg Al-WTR (Figure 4e) was a removed 69.2% of PO$_4$ and had limited c$_e$ in solution. Bai et al. (2017) found that physical sorption was dominant mechanism at low spiked concentrations. Physical sorption in conjunction with lower temperature would contribute to the higher amounts of PO$_4$ released during desorption.
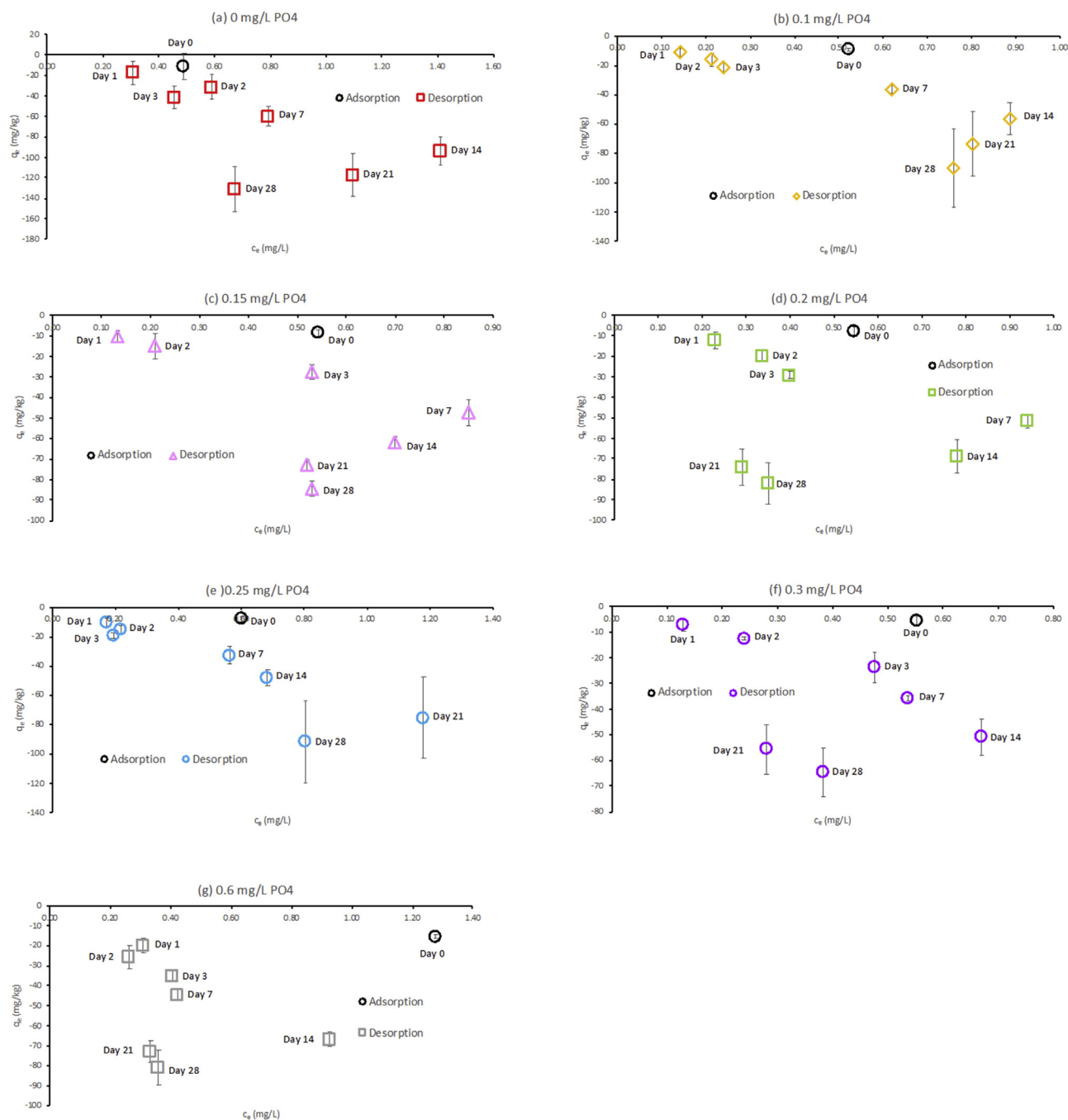
3.3. Fe-WTR adsorption-desorption isotherms

The Fe-WTR originated from a drinking water facility where the surface water has an average PO$_4$ concentration of 0.02–0.03 mg/L. As FeCl$_3$ was also shown to have a high affinity toward phosphorus species (Shi et al., 2011), it was not surprising that only the control set of distilled water adsorption phase experiments released previously adsorbed PO$_4$. All the spiked conditions adsorbed PO$_4$, with the sorption phase q$_e$ increasing with increasing spiked concentration (Figure 5a). A similar phenomenon was exhibited when surface water at 20 °C (Figure 5b) or 5 °C (Figure 5c) was used as the background solution. The surface water

used for 20 °C and 5 °C experiments contained 0.01 mg/L PO$_4$ and 0.03 mg/L PO$_4$in the background solution, respectively. Other researchers had found that more PO$_4$ would adsorb to iron based materials at 20 °C than lower temperatures (Choi et al., 2016). The slight increase in the PO$_4$ surface water content was enough to offset the impact from the colder temperature, leading to 20 °C and 5 °C conditions having similar q$_e$ values (p > 0.05).

During the desorption phase, experiments that used distilled water as the background solution continued to release previously bound PO$_4$. As with the Al-WTR, this was more pronounced at the lower spiked concentrations. The 0.25 mg/L PO$_4$ spiked condition maintained a positive q$_e$ only for the first three days (Figure 6e). Only the 0.6 mg/L PO$_4$ spiked condition continued to retain appreciable levels of sorbed PO$_4$. However, the 9.33 mg/kg Fe-WTR that had adsorbed during the 24 h adsorption phase had decreased to 2.68 mg/kg Fe-WTR after 28 days of desorption (Figure 6g).

The presence of 0.1 mg/L PO$_4$ in the surface water used as background solution helped to mitigate the impact of the reverse concentration gradient effect. For example, the 0.26 mg/L spiked + surface water (Figure 7e) and did not desorb significant amounts (p < 0.05) of PO$_4$ until the 14 day desorption step while the 0.31 mg/L spiked (0.30 mg/L)+surface water (0.01 mg/L) (Figure 7f) only desorbed significant amounts on the 21 day desorption step. Although the 0.61 mg/L spiked +

Figure 10. Ferrous-WTR (Fe2-WTR) batch desorption isotherms with distilled water and stored statically at 20 °C for initial spiked PO4 concentration of: a) Control (0 mg/L spiked PO4); b) 0.10 mg/L spiked PO4; c) 0.15 mg/L spiked PO4; d) 0.20 mg/L spiked PO4; e) 0.25 mg/L spiked PO4; f) 0.30 mg/L spiked PO4; asnd g) 0.6 mg/L PO4. Error bars are standard deviation of the triplicate samples. Data labels corresponds to the cumulative desorption day (i.e., d21 is cumulative desorption by day 21).

Table 1. Aqueous PO_4 values (c_e) and cumulative desorption of PO_4 at day 3, 7 and 14 using Fe2-WTR with surface water containing 1.306 mg/L of PO_4. Standard deviations are based on three replicates. Note: negative qe indicates amount desorption of PO_4 bound during in plant coagulation.

Spiked + surface water PO4 (mg/L)	Day 3		Day 7		Day 14	
	c_e (mg/L)	q_e (mg/kg)	c_e (mg/L)	q_e (mg/kg)	c_e (mg/L)	q_e (mg/kg)
1.306	2.77	-56.9 ± 26.1	3.07	-94 ± 18.8	4.65	-194.8 ± 30.9
1.406	2.44	-70.1 ± 33.1	4.22	-135.3 ± 35.9	4.92	-243.6 ± 95.6
1.456	3.05	-71.7 ± 25.5	4.58	-144.0 ± 20.0	5.23	-227.7 ± 16.7
1.506	2.26	-29.9 ± 6.7	3.40	-199.6 ± 49.3	3.40	-119.6 ± 49.3
1.556	3.01	-57.4 ± 36.5	3.58	-104.8 ± 15.7	4.69	-178.4 ± 15.9
1.606	2.39	-56.5 ± 6.7	4.25	-120.2 ± 12.6	4.87	-196.2 ± 15.7
1.906	2.19	-31.8 ± 5.1	3.74	-86.7 ± 17.3	4.48	-156.1 ± 10.4

Table 2. Coefficients of Langmuir and Freundlich adsorption isotherm models. (Negative values are indicative of the desorption of previously bound PO_4 form the WTR).

	Condition	Langmuir			Freundlich		
		q_m (mg/kg WTR)	K_{ads} (L/mg)	R^2	1/n	K	R^2
Al-WTR	Distilled water, 20 °C	16.95	73.75	0.83	0.50	1.01	0.94
	Surface water, 20 °C	6.64	55.56	0.63	0.08	2.27	0.02
	Surface water, 5 °C	4.45	192.31	0.26	0.07	1.50	0.02
Fe-WTR	Distilled water, 20 °C	0.11	-0.52	0.44	0.06	0.97	0.82
	Surface water, 20 °C	-10.50	35.84	0.38	0.54	0.92	0.88
	Surface water, 5 °C	5.06	-156.25	0.009	0.29	1.37	0.20
Fe2-WTR	Distilled water, 20 °C	-2.66	7.49	0.31	Not mathematically valid calculation		
	Surface water, 20 °C	0.12	0.10	0.32	Not mathematically valid calculation		

surface water concentration yielded a 28 day cumulative desorption q_e of 5.67 mg/kg Fe-WTR (Figure 7g), it was significantly higher ($p < 0.05$) than that obtained when distilled water was used (Figure 6g).

The same general trend was exhibited with surface water that was incubated at 5 °C experiment. As the spiked + surface water PO_4 concentration increased, the extent of desorption decreased (Figure 8). This was evident by all but the control (Figure 8a) and 0.13 spiked + surface water (Figure 8b) being able to retain the adsorbed PO_4 during the extended desorption steps. Therefore Fe-WTR would not be recommend for use at colder temperatures.

3.4. Fe2-WTR adsorption-desorption isotherms

As with the other WTRs, Fe2-WTR released previously bound PO_4 during the initial 24 h adsorption (Figure 9a). However, the amount of PO_4 released during the adsorption phase was significantly higher than with Al-WTR or Fe-WTR ($p < 0.05$). The larger particle size of Fe2-WTR contributed to the lower sorption capacity. Caporale et al. (2013) reported a lower sorption of arsenic on Fe-based WTR due to the lower surface area. However, the primary reason of decreased sorption capacity was attributed to the substantially higher levels of PO_4 removed during the coagulation process. Wastewater from cheese manufacture can contain more than 3000 mg/L PO_4 (Guerreiro et al., 2020). When surface water containing an initial 1.31 mg/L PO_4 was used as the background solution (Figure 9b), positive q_e values were obtained only for spiked + surface water concentrations greater than 1.46 mg/L PO_4.

Although some spiked PO_4 concentrations could be adsorbed by Fe2-WTR, the desorption phase was more significant (<0.05). With distilled water as the background solution, desorption was more pronounced at lower spiked conditions ($p < 0.05$). Figure 10a shows that the cumulative 28 day qe released 131 mg PO_4/kg Fe2-WTR for the control while the 0.3 mg/L PO_4 spiked condition (Figure 10f) only released 64 mg PO_4/kg Fe2-WTR ($p < 0.05$). Even when surface water containing 1.306 mg/L of PO_4 was used, the Fe2-WTR continued to release PO_4 (Table 1). These results indicated that additional sorption was not possible with this WTR. Gibbons and Gagnon (2011) found that differences in adsorption tied to the mass of primary element left in the solid. A review by Xu et al. (2020) reported that effective removal was possible for Fe-WTRs that contained 170 g total Fe/kg WTR. Therefore, if an excess dose was not used during the coagulation application that generated the Fe2-WTR, the remaining Fe content may have been insufficient for adsorbing PO_4.

3.5. Comparison of WTRs

Alum -WTR was shown to selectively adsorb PO_4 (Yang et al., 2006). The Al-WTR adsorption isotherms yielded higher Langmuir and Freundlich K values than Fe- or Fe2-WTRs (Table 2). This selectivity was why Al-WTR depicted a higher overall adsorption than Fe-WTR, even when other constituents were present (i.e., surface water as background solution). An earlier study with arsenate, an analogue of phosphate, also

indicated that Al-WTR was more effective than Fe-WTR at a wide range of pH values (Nagar et al., 2010). However other researchers had conflicting results. For instance, de Sousa et al. (2012) documented that mesoporous spheres containing Al-oxide and or Fe-oxides preferentially bound to Fe sites. Castaldi et al. (2014) also found similar Fe-WTR to be more effective than Al-WTR. The change could in adsorption effectiveness was most likely due to the specific constituents present in each surface water. The study by Nagar et al. (2010) indicated that sulfate would not have a significant impact on either WTR. Conversely, low molecular weight organic acids could interfere with initial PO_4 sorption to alum-ferric WTRs (Oliver et al., 2011). The level of natural organic matter in the surface water used in the study may have resulted in Al-WTR being more effective.

Unlike Al-WTR, Fe-WTR surface water results were better represented by the Freundlich model than the Langmuir model. The surface water experiments 1/n (Table 2) at 20 °C (0.54) and 5 °C had indicated a higher sorption than when distilled water was used (0.06) (Cheng et al., 2017; Gao et al., 2013). Ferric based WTRs may have more intraparticle diffusion (Gibbons and Gagnon, 2011) which could result in higher removal efficiencies with high PO_4 concentrations. This was corroborated by the 0.6 mg/L PO_4 spiked concentration exhibiting the most adsorption and least desorption. Extent of sorption would also depend on if WTR was used as a sludge (i.e., not processed) or sieved prior to use (Brennan et al., 2011). Neither the Al-WTR or Fe-WTR were sieved prior to use. However, the Fe-WTR initially contained more water and had to be air-dried before use. The drying process increased the final particle size which might have negatively impacted its effectiveness.

Ferrous sulfate based WTR (Fe2-WTR) exhibited the worst overall performance for this study. The amount of previously bound PO_4 (during coagulation operations) that desorbed prevented the data from being modeled with the Freundlich equation (Table 2). Although K_{ads} for the Langmuir equation was calculated, the R^2 was too low to be considered good fit which rendered the K_{ads} to be an unrealistic number (Khayyun and Mseer, 2019). Ferrous sulfate is often used in as a coagulant in wastewater applications as it is cheaper than ferric chloride. However, as was shown in Eq. (4), once dosed it undergoes a two-step reaction to form the iron hydroxide needed to react with inorganic constituents. Either inadequate time for the reaction to complete, not applying an excess $FeSO_4$ dose or extremely high initial contaminant levels rendered the Fe2-WTR used in this study ineffective for additional removal of PO_4.

4. Conclusions

Al-WTR yield the most significant adsorption q_e ($p < 0.05$) and least amount of desorption for the conditions studied. Adsorption by iron-based WTRs appeared to be more susceptible to the reverse concentration gradient effect, particularly at PO_4 concentrations <0.25 mg/L. The PO_4 content in surface water mitigated some of the effect. Full potential was not evident as the background PO_4 in the Fe-WTR surface waters was

low. Additional experiments would need to be conducted to determine if Fe-WTR could be used to remove PO_4 from other surface waters. Although this research focused on PO_4, it is recommended that the potential desorption of nitrates and inorganics from the WTRs be assessed prior to using the WTRs in field. The specific compounds to track will depend on constituents were present in the source water.

Declarations

Author contribution statement

George Carleton: Performed the experiments; Analyzed and interpreted the data; Wrote the paper.

Haidar Al daach: Performed the experiments; Analyzed and interpreted the data.

Teresa J. Cutright: Conceived and designed the experiments; Performed the experiments; Contributed reagents, materials, analysis tools or data; Wrote the paper.

Funding statement

Competing interest statement

The authors declare no conflict of interest.

Additional information

No additional information is available for this paper.

References

Ahmad, T., Ahmad, K., Alam, M., 2017. Sludge quantification at water treatment plant and its management scenario. Environ. Monit. Assess. 189, 453–463.

Ashekuzzaman, S.M., Ferrestal, P., Richards, K., Fenton, O., 2019. Dairy industry derived wastewater treatment sludge: generation type, and characterization of nutrients and metals for agricultural reuse. J. Clean. Prod. 230, 1266–1275.

Bacelo, H., Pintor, A.M.A., Santos, S.C.R., Boaventura, R.A.R., Botelho, C.M.S., 2020. Performance and prospects of different adsorbents for phosphorus uptake and recovery from water. Chem. Eng. J. 381, 122566.

Bai, J., Ye, X., Jia, J., Zhang, G., Zhao, Q., Cui, B., Liu, X., 2017. Phosphorus sorption-desorption and effects of temperature, pH and salinity on phosphorus sorption in marsh soils from coastal wetlands with different flooding conditions. Chemosphere 188, 677–688.

Brennan, R.B., Fenton, O., Rodgers, M., Healy, M.G., 2011. Evaluation of chemical amendments to control phosphorous losses from dairy slurry. Soil Use Manag. 27, 238–246.

Caporale, A.G., Punamiya, P., Pigna, M., Violante, A., Sarkar, D., 2013. Effect of particle size of drinking-water treatment residuals on the sorption of arsenic in the presence of competing ions. J. Hazard Mater. 260, 644–651.

Carvalho, R., Prazeres, A.R., Rivas, J., 2013. Chees whey wastewater: characterization and treatment. Sci. Total Environ. 445–446, 385–396.

Castaldi, P., Mele, E., Silvetti, M., Garau, G., Deiana, S., 2014. Water treatment residues as accumulators of oxoanions in soil. Sorption of arsenate and phosphate anions from an aqueous solution. J. Hazard Mater. 264, 144–152.

Cheng, Q., Li, H., Xu, Y., Chen, S., Liao, Y., Deng, F., Li, J., 2017. Study on the adsorption of nitrogen and phosphorus from biogas slurry by NaCl-modified zeolites. PloS One 12 (5), e0176109.

Choi, J., Chung, J., Lee, W., Km, J.O., 2016. Phosphorous adsorption on synthesized magnetite in wastewater. J. Ind. Eng. Chem. 34, 198–203.

Corwin, C.J., Summers, R.S., 2011. Adsorption and desorption of trace organic contaminants from granular activated carbon adsorbers after intermittent loading and through backwash cycle. Water Res. 45, 417–426.

Dayton, E.A., Basta, N.T., 2001. Characterization of drinking water treatment residuals for use as a soil substitute. Water Environ. Res. 73, 52–57.

de Sousa, A.F., Braga, P.T., Gomes, E.C.C., Valentini, A., Longhinotti, E., 2012. Adsorption of phosphate using mesoporous spheres containing iron and aluminum oxides. Chem. Eng. J. 210, 143–149.

Ebeling, J.M., Sibrell, P.L., Ogden, S.R., Summerfelt, S.T., 2003. Evaluation of chemical coagulation-flocculation aids for the removal of suspended solids and phosphorous for intensive recirculating aquaculture effluent discharge. Aquaculture Engineering 29, 23–42.

Gao, S., Wang, C., Pei, Y., 2013. Comparison of different phosphate species adsorption by ferric and alum water treatment residuals. J. Environ. Sci. 25 (5), 986–992.

Gibbons, M.K., Gagnon, G.A., 2011. Understanding removal of phosphate or arsenate onto water treatment residual solids. J. Hazard Mater. 186, 1916–1923.

Guerreiro, R.C.S., Jeronimo, E., Luz, S., Pinheiro, H.M., Prazeres, A.R., 2020. Cheese manufacturing wastewater treatment by combined physicochemical processes for reuse and fertilization production. J. Environ. Manag. 264, 110470.

HACH DR 890 Procedures Manual, 2009. hach.com.

Hale, S.E., Alling, V., Martinsent, V., Mulder, J., Breedveld, G.D., Croneilissen, G., 2013. The sorption and desorption of phosphate-P, ammonium-N and nitrate-N n cacao shell and corn cob biochars. Chemosphere 91, 1612–1619.

Ippolito, J.A., 2015. Aluminum-based water treatment residual use in a constructed wetland for capturing urban runoff phosphorus: column study. Water Air Soil Pollut. 226, 334–344.

Khayyun, T.S., Mseer, A.H., 2019. Comparison of the experimental results with Langmuir and Freundlich models for copper removal on limestone adsorbent. Applied Water Science 9, 170–179.

Li, S., Jiang, F., Lei, T., Ren, Z., Wang, S., Yang, X., 2019. Phosphorus removal by in situ sprayed ferric chloride in Dianchi Lake: efficiency, stability, and mechanism. Process Saf. Environ. Protect. 131, 320–328.

Maiz, I., Esnaola, V., Millan, E., 1997. Evaluation of heavy metal availability in contaminated soils by a short extraction procedure. Sci. Total Environ. 206, 107–115.

Matilainen, A., Vepsalainen, M., Sillanpaa, M., 2010. Natural organic matter removal by coagulation during drinking water treatment a review. Adv. Colloid Interface Sci. 159, 189–197.

Nagar, R., Sarkar, D., Markis, K.C., Datta, R., 2010. Effect of solution chemistry on arsenic sorption by Fe- and Al-based drinking-water treatment residuals. Chemosphere 78, 1028–1035.

Oliver, I.W., Grant, C.D., Murray, R.S., 2011. Assessing effects of aerobic and anaerobic conditions on phosphorous sorption and retention capacity of water treatment residuals. J. Environ. Manag. 92, 960–966.

Razali, M., Zhao, Y.Q., Bruen, M., 2007. Effectiveness of a drinking-water treatment sludge in removing different phosphorus species from aqueous solution. Separ. Purif. Technol. 55, 300–306.

Reynolds, T.D., Richards, P.A., 1996. Unit Operations and Processes in Environmental Engineering. PWS Publishing, Boston, MA.

Rivas, J., Prazeres, A.R., Carvalho, F., Beltran, F., 2010. Coagulation-flocculation and aerobic biodegradation. J. Agric. Food Chem. 58, 7871–7877.

Shi, Z.L., Liu, F.M., Yao, S., 2011. Adsorptive removal of phosphate from aqueous solution using activate carbon loaded with Fe(III) oxide. N. Carbon Mater. 26 (4), 299–306.

Turner, T., Wheeler, R., Stone, A., Oliver, I., 2019. Potential alternative reuse pathways for water treatment residuals: remaining barriers and questions – a review. Water Air Soil Pollut. 230, 227–257.

United States Environmental Protection Agency (USEPA), 2011. Drinking Water Treatment Plant Residuals Management Technical Report. Summary of Residuals Generation, Treatment and Disposal at Large Community Water Systems. EPA 820-R-11-003.

United States Environmental Protection Agency (USEPA), 2018. Aquatic Life Ambient Water Quality Criteria for Aluminum in Freshwater. EPA-822-R-18-001.

Wang, C.H., Gao, S.J., Wang, T.X., Tian, B.H., Pei, Y.S., 2011. Effectiveness of sequential and acid activation on phosphorus removal by ferric and alum water treatment residuals. Chem. Eng. J. 172, 885–891.

Wang, C., Jiang, H., Yuan, N., Pei, Y., Yan, Z., 2016. Tuing the adsorptive properties of drinking water treatment residue via oxygen-limited hat treatment for environmental recycle. Chem. Eng. J. 284, 571–581.

Xu, D., Lee, L.Y., Lim, F.Y., Lyu, Z., Zhu, H., Ong, S.L., Hu, J., 2020. Water treatment residual: a critical review of its applications on pollutant removal from stormwater runoff and future perspectives. J. Environ. Manag. 259, 109649.

Yang, Y., Zhao, Y.Q., Babatunde, A.O., Wang, L., Ren, Y.X., Han, Y., 2006. Characteristics and mechanisms of phosphate adsorption on dewatered alum sludge. Separ. Purif. Technol. 51, 193–200.

Zohar, I., Ippolito, J.A., Massey, M.S., Litaor, I.M., 2017. Innovative approach for recycling phosphorous form agro-wastewaters using water treatment residuals (WTR). Chemosphere 168, 234–243.